Proton glass behavior and hopping conductivity in solid solutions of antiferroelectric betaine phosphate and ferroelectric betaine phosphite

S. L. Hutton, I. Fehst, R. Böhmer, M. Braune, B. Mertz, Peter Lunkenheimer, Alois Loidl

Angaben zur Veröffentlichung / Publication details:

Hutton, S. L., I. Fehst, R. Böhmer, M. Braune, B. Mertz, Peter Lunkenheimer, and Alois Loidl. 1991. "Proton glass behavior and hopping conductivity in solid solutions of antiferroelectric betaine phosphate and ferroelectric betaine phosphite." *Physical Review Letters* 66 (15): 1990–93. https://doi.org/10.1103/physrevlett.66.1990.

Proton Glass Behavior and Hopping Conductivity in Solid Solutions of Antiferroelectric Betaine Phosphate and Ferroelectric Betaine Phosphite

S. L. Hutton, I. Fehst, R. Böhmer,[a] M. Braune, B. Mertz, P. Lunkenheimer, and A. Loidl
Institut für Physik, Universität Mainz, D-6500 Mainz, Federal Republic of Germany
(Received 29 October 1990)

Measurements of the dielectric permittivity are reported for solid solutions of antiferroelectric betaine phosphate and ferroelectric betaine phosphite at frequencies 10^{-2} Hz $< \nu <$ 10^{9} Hz and temperatures 2 K $< T <$ 300 K. In these compounds the inorganic components are linked by hydrogen bonds to one-dimensional chains. The mixed crystal with a phosphate concentration $x=0.95$ orders antiferroelectrically at $T_c=79$ K. For $T > T_c$ the dielectric response is dominated by ac and dc conduction. The 40% sample exhibits pure relaxational behavior indicative of a transition into an orientational glass state.

PACS numbers: 61.42.+h, 64.70.Pf, 72.20.−i, 77.40.+i

Betaine phosphate [BP: $(CH)_3NCH_2COO\cdot H_3PO_4$] and betaine phosphite [BPI: $(CH)_3NCH_2COO\cdot H_3PO_3$] are molecular crystals of the amino-acid betaine and the phosphoric or the phosphorous acids, respectively. In both compounds the inorganic components (PO_4 or PO_3 groups) are linked by hydrogen bonds to quasi-one-dimensional chains.[1] BP exhibits a ferroelastic transition near 365 K followed by two phase transitions at 86 and 81 K.[1] Antiferroelectric (AFE) order is established at $T_c=86$ K.[2] At this temperature the O-H $\cdots$ O bonds order along the one-dimensional chains and the chains are linked antiferroelectrically.[3] At 355 K BPI transforms into an elastically ordered state and exhibits ferroelectric (FE) order below $T_c=216$ K.[1,4] The two almost isostructural compounds form solid solutions at any concentration.[4] It has been shown recently that at intermediate concentrations the long-range electric order is suppressed.[5]

BP:BPI single crystals were supplied by J. Albers (Fachbereich Physik, Universität des Saarlandes, Federal Republic of Germany). The crystals were grown by controlled evaporation from aqueous solutions. For the dielectric spectroscopy gold-plated single crystals were oriented along the monoclinic b axis. To cover the broad range of frequencies three different experimental setups were used: a frequency response analyzer supplemented with a high-impedance preamplifier allowed measurements from 10^{-2} to 10^{4} Hz. In the audio-frequency range automated low-frequency bridges were used. These experiments were performed in home-manufactured variable-flow ^{4}He cryostats (2 K $\leq T \leq$ 300 K). The high-frequency data were recorded using an HP 4191A impedance analyzer connected to a refrigerator system via an air line.[6]

In all experiments the capacitance $C(\omega,T)=C_0\varepsilon'(\omega,T)$ and conductance $G(\omega,T)=C_0\sigma(\omega,T)/\varepsilon_0$ were recorded. C_0 is the geometrical capacitance, ε' the real part of the dielectric constant, σ the real part of the conductivity, ε_0 the dielectric permittivity of free space (8.85×10^{-12} F/m), and $\omega=2\pi\nu$, the angular frequency. The complex dielectric constant ε^* as well as the complex conductivity σ^* can be calculated from C and G. In particular, the imaginary part of the dielectric constant $\varepsilon''(\omega,T)=G(\omega,T)/\omega C_0=\varepsilon_0\sigma(\omega,T)/\omega$.

For BP:BPI(40), no anomaly in $\varepsilon'(T)$ indicative of a polar phase transition can be detected down to the lowest temperatures.[5] Instead, for $T < 30$ K dispersion effects dominate the dielectric response. Results are shown in Fig. 1. Here the real and the imaginary parts of the dielectric constant, ε' and ε'', respectively, are plotted versus the logarithm of the measuring frequency $\log_{10}(\nu)$ for different temperatures. The experimental results of Fig. 1 provide clear evidence that ε'' vs $\log_{10}(\nu)$ is asymmetric and polydispersive. The width is much broader than 1.14 decades expected for a monodispersive Debye relaxator.

The freezing phenomena in BP:BPI(40) reveal the characteristics of a transition into a dipolar glass state: The slowing down of the dipolar degrees of freedom exhibits broad and asymmetric distributions of the relaxation rates, with a width of the distribution exceeding by orders of magnitude the width of a monodis-

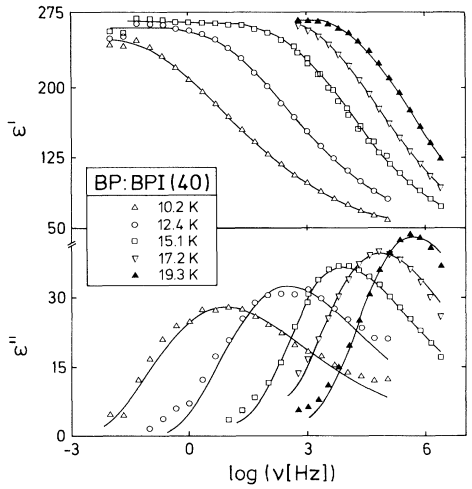

FIG. 1. Dielectric constant ε' and dielectric loss ε'' vs the logarithm of the measuring frequency $\log_{10}(\nu)$ in BP:BPI(40). The solid lines are fits with the Fourier transform of the KWW function.

persive Debye process.[7] Dipolar glasses, a subspecies of orientational glasses (OG),[7] have been studied in detail; the most prominent examples are KCl:OH^-,[8] $K_{1-x}Li_xTaO_3$,[9] and the archetypical proton glass $Rb_{1-x}(NH_4)_xH_2PO_4$ (RADP).[10] In OG the reorienting moments freeze into random configurations.[7] The interplay of site disorder and frustrated interactions is responsible for the freezing transition which bears similarities with the spin-glass transition in dilute magnetic systems[11] and with the relaxation dynamics in canonical glasses.[12]

We fitted the data with the (semi-infinite) Fourier transform $\mathcal{F}$ of the Kohlrausch-Williams-Watts[13] (KWW) function which describes stretched exponential behavior in the time domain: $\Phi(t) \approx \exp[-(t/\tau_{KWW}) \times \beta_{KWW}]$. τ_{KWW} is a characteristic relaxation time and β_{KWW} the fractional exponent. The best fits using $\varepsilon(\omega,T) = \varepsilon_\infty + 4\pi\chi_s \mathcal{F}\, d\Phi/dt$ are indicated as solid lines in Fig. 1. The temperature dependence of the fit parameters, namely, the static susceptibility χ_s, the fractional exponent β_{KWW}, and the relaxation rate $\tilde{\nu} = 1/2\pi\tau_{KWW}$ are shown in Fig. 2.

Figure 2(a) reveals a cusp in χ_s near 20 K. It is calculated from the area of the loss peak and corresponds to the static susceptibility in the paraelectric phase only. Below the glass transition temperature, when strong nonequilibrium effects become important, any extrapolation to zero frequency is highly speculative and must fail. β_{KWW} is small, corresponding to a high asymmetry and decreases with decreasing temperatures [Fig. 2(b)]. Finally, the relaxation rate follows an Arrhenius-type behavior suggesting that the characteristic relaxation time exhibits a divergence for $T=0$ K only [Fig. 2(c)]. A best fit with an Arrhenius equation, $\nu = \nu_0 \exp(-E_b/k_BT)$ is indicated in Fig. 2(c) by a solid line. The attempt frequency $\nu_0 = 0.28$ THz and is of the order of a phonon or librational frequency. The hindering barrier $E_b = 252$ K. We suggest that deviations from purely thermally activated behavior either signal the onset of nonequilibrium effects at low T or indicate the increasing importance of tunneling transitions at low temperatures. The appearance of quantum fluctuations has also been reported for the orientational glass KI:NH_4I.[14]

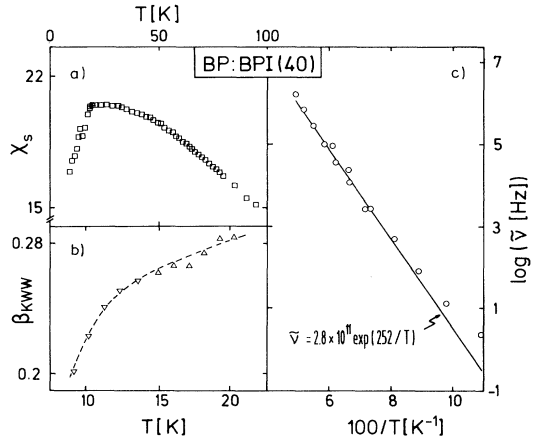

FIG. 2. Temperature dependence of the parameters of the KWW fits to the experimental data in BP:BPI(40): (a) static susceptibility χ_s, (b) shape parameter β_{KWW}, and (c) characteristic relaxation rate $1/2\pi\tau_{KWW}$ vs $1/T$. The solid line in (c) corresponds to a thermally activated behavior with an attempt frequency $\nu_0 = 2.8 \times 10^{11}$ Hz and a hindering barrier $E_b = 252$ K. The dashed lines in (a) and (b) are drawn to guide the eye.

As in the OG state of RADP,[10] the competing FE and AFE interactions are responsible for the glassy low-temperature state: In RADP the acid protons form a three-dimensional network of O-H $\cdots$ O bonds. At the glass transition the protons freeze at random in the double-minimum potentials.[10] By analogy we conclude, that in BP:BPI(40), due to the substitutional disorder, the protons freeze in their double-well potentials along the one-dimensional chains devoid of long-range order. However, the freezing dynamics in BP:BPI(40) shows distinct differences to what is observed in RADP: In the latter system the temperature dependence of the mean relaxation times can be parametrized in terms of a Vogel-Fulcher law with a "static" Vogel-Fulcher temperature $T_{VF} \approx 8$ K. The distribution of relaxation times is symmetrically shaped and can be explained in terms of a distribution of energy barriers.[7,10]

The mean relaxation rates in BP:BPI(40) follow a thermally activated temperature dependence. A relaxation behavior which can be parametrized by energy barriers exceeding by orders of magnitude the Vogel-Fulcher temperature is a common feature of all orientational glasses.[7,15] It closely resembles the freezing dynamics of the primary relaxation in "strong" glasses.[16] Strong glasses show an almost pure Arrhenius-like relaxation. In addition, heat-capacity experiments in BP:BPI(40) exhibit no anomaly.[17] Strong glasses have a low density of configurational states in their potential-energy surface.[16] Accordingly, this low degeneracy is thought to be responsible for the lack of a heat-capacity anomaly at the glass transition. It has been suggested that the natural separation of time scales for reorientational and translational motions is responsible for the strong character of OG.[15]

At a first glance, the experimental results in BP:BPI(40) seem to be at odds with the pure coupling model as developed by Ngai and co-workers.[18] This model predicts deviations from an Arrhenius behavior whenever β_{KWW} is T dependent or ν_0 is much larger than a typical phonon frequency. However, by combining coupling and site disorder, the experimental results may well be consistent with theory.[19]

Finally, we would like to compare the temperature dependence of χ_s [Fig. 2(a)], β_{KWW} [Fig. 2(b)], and $\tilde{\nu}$ [Fig. 2(c)] with results from computer simulations. Monte Carlo calculations in OG predict static glass transition temperatures at zero temperature and glasslike slow relaxations consistent with the KWW law and with

a strongly temperature-dependent β_{KWW}.[20]

For all concentrations, except for $x=0.95$, the complex dielectric constant ε^* can be interpreted taking only relaxational phenomena into account. BP:BPI(95) behaves totally different: As will be shown below, in this compound the dielectric response bears the signature of pure ac and dc conduction.

BP:BPI(95) shows AFE order below $T_c=79$ K.[5] The dielectric loss $\varepsilon''(\nu,T)$ clearly indicates the presence of partially mobile charge carriers: Starting from high frequencies, the loss increases smoothly with decreasing frequencies with a steeply rising branch towards low frequencies. Figure 3 shows the conductivity $\sigma\approx\omega\varepsilon''$ versus the frequency ν on a log-log scale for different temperatures above and below the AFE phase transition. These experimental results clearly reveal the limiting dc conductivity at low frequencies and the sublinear power-law behavior of σ with increasing frequencies. For $\nu>100$ MHz dispersion effects due to relaxation processes become apparent which appear in addition to the conductivity. And indeed, for pure BP a single Debye relaxation has been measured with a relaxation rate $\nu=380$ GHz (300 K) and $\nu=135$ GHz (140 K).[21] In Fig. 3(a), $\varepsilon''(T)$ is plotted for different measuring frequencies. It demonstrates that the dielectric loss and the corresponding ac conduction are reduced by an order of magnitude at the AFE ordering temperature.

The conductivity data of Fig. 3 were fitted using $\sigma(\omega)=\sigma_{dc}+A\omega^s$, a parametrization which is frequently used.[22] The results of the best fits are indicated as solid lines. Slight deviations from the simple power-law behavior appear in the audio-frequency range. This is more clearly resolved by plotting $\tilde{\varepsilon}''=(\sigma-\sigma_{dc})/\omega$ vs $\log_{10}(\nu)$ [Fig. 3(b)]. Figure 3(b) reveals that at high T, contributions due to ac conductivity are dominant, but in addition a weak relaxation process can be located. For $T<T_c$ the ac conductivity is weak and the relaxation mode is clearly separated.

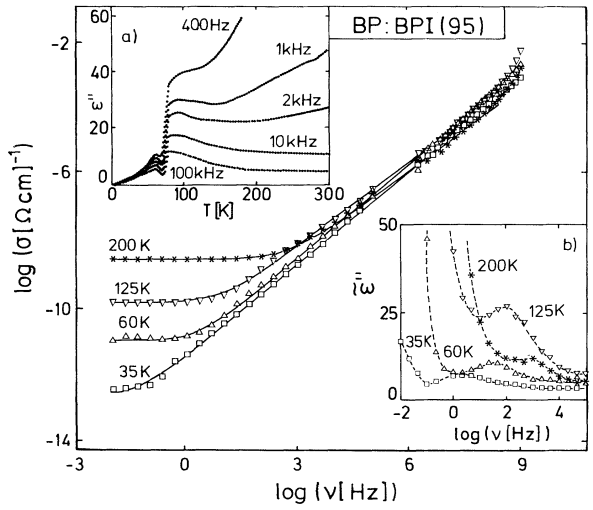

FIG. 3. Logarithm of the conductivity [$\log_{10}(\sigma)$] vs $\log_{10}(\nu)$ in BP:BPI(95) at different temperatures above and below the antiferroelectric phase transition $T_c=79$ K. The solid lines are fits to the data as described in the text. (a) Temperature dependence of the dielectric loss ε'' vs T at different measuring frequencies. (b) Frequency dependence of the dielectric loss after subtracting the dc conductivity vs $\log_{10}(\nu)$.

The temperature dependence of the parameters of the best fits to the conductivity data are shown in Fig. 4. With decreasing temperatures the amplitude A of the ac conductivity slightly increases and exhibits an abrupt decrease of an order of magnitude below the AFE phase transition [Fig. 4(a)]. The frequency exponent s exhibits a drop from almost 1 for $T<T_c$ to 0.85 for $T>T_c$ and then slightly decreases for further increasing T [Fig. 4(b)]. The data provide clear evidence that the ac conductivity is suppressed by the onset of long-range AFE order and, thus, that the ac conductivity is triggered by the proton dynamics.

Pollak and Pike[23] have proposed a model for the ac conductivity of glasses due to atomic hopping between sites with random space and energy separations. They found that glassy materials should generally show a nearly linear frequency-dependent conductivity. This type of linear frequency dependence is obtained any time the distribution of relaxation times varies very smoothly on a logarithmic scale. Deviations from linearity are due to specific conductivity mechanisms. A possible conduction mechanism in BP:BPI(95) is charge transfer via correlated barrier hopping (CBH).[22,24] In the CBH

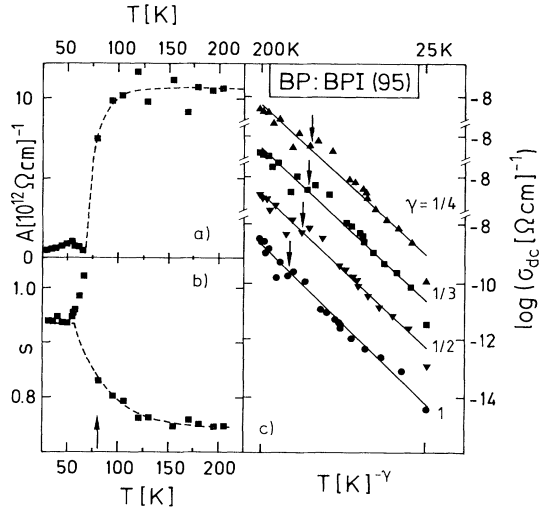

FIG. 4. Temperature dependence (a) of the amplitude of the ac conductivity A, (b) of the T dependence of the frequency exponent s, and (c) of the dc conductivity. The dc conductivity has been plotted vs $T^{-\gamma}$ ($\gamma=1$, $\frac{1}{2}$, $\frac{1}{3}$, and $\frac{1}{4}$). Note that the temperature scale is different for each set of data; the limiting high and low temperatures of each plot corresponds to 200 and 25 K, respectively. T_c for each set of data is indicated by an arrow. The solid lines are fits using $\sigma_{dc}\approx\exp[-(\text{const}/T^{\gamma})]$. The χ^2 relative to that with $\gamma=1$ are $\gamma=\frac{1}{2}$, 1.45; $\gamma=\frac{1}{3}$, 2.02; and $\gamma=\frac{1}{4}$, 2.37.

model, charge carriers are assumed to hop between sites, separated by potential barriers with a random height distribution. The frequency exponent s is predicted to be 1 at low temperatures and to decrease smoothly with increasing temperatures. $s(T)$ as observed in BP:BPI(95) [Fig. 4(b)] closely resembles this behavior.

In addition, the CBH model predicts a relaxation at audio frequencies which is due to a limiting critical frequency ν_c. This critical relaxation rate corresponds to the highest energy barrier that has to be crossed.[24] ν_c should be thermally activated following the same Arrhenius behavior as the dc conduction.[24] A rough estimate of the energy barriers as calculated from the temperature dependence of the peak maxima in Fig. 3(b) yields $E_b \approx 200$ K.

The temperature dependence of the dc conductivity is shown in Fig. 4(c). Here we used a representation $\log_{10}(\sigma_{dc})$ vs $T^{-\gamma}$ to account for different models for the temperature dependence of $\sigma_{dc} \approx \exp[-(\text{const}/T)^{\gamma}]$. For electronic processes, the variable-range-hopping (VRH) models[25] predict, depending on the dimensionality, $\gamma = \frac{1}{4}$ (3D), $\gamma = \frac{1}{3}$ (2D), and $\gamma = \frac{1}{2}$ (1D). If the dc conductivity is due to thermally activated processes of charge carriers, Arrhenius behavior ($\gamma = 1$) would result. The solid lines in Fig. 4(c) correspond to the best fits. The quality of the fits points towards a thermally activated process with a hindering barrier $E_b = 464$ K. This value is only of the order of magnitude as the barrier determined from the relaxation in the audio-frequency range. An important observation seems to be the fact that the dc conductivity is not influenced by the AFE phase transition which allows two possible interpretations: (i) ac and dc conductivities are of different origin or (ii) the limiting barriers for dc conduction are not influenced by the AFE phase transition.

In conclusion, we provided compelling evidence that BP:BPI(40) exhibits an OG state at low temperatures, with the protons frozen-in along one-dimensional chains. The loss peaks [ε'' vs $\log_{10}(\nu)$] are anomalously broad indicating a broad distribution of relaxation times. At audio frequencies BP:BPI(95) is governed by ac conduction indicating hops of charge carriers (protons) over energy barriers with a random height distribution. The low-frequency response is dominated by dc conduction which is thermally activated. Solid solutions of BP:BPI reveal, depending on the strength of competing interactions and on the degree of substitutional disorder, polar order (pure compounds), glassy relaxational behavior (at intermediate concentrations), and pure conductivity phenomena (for low substitutional disorder). (Systematic studies should allow for a unified view of these phenomena.)

We thank C. A. Angell, K. Binder, K. Funke, and K. L. Ngai for illuminating discussions and useful comments on the manuscript. This work was supported by the Sonderforschungsbereich No. 262 (Mainz) and the Center for Materials Research (Materialwissenschaftliches Forschungszentrum Mainz).

[a]Present address: Department of Chemistry, Arizona State University, Tempe, AZ 85287.

[1]J. Albers, Ferroelectrics **78**, 3 (1988); G. Schaack, Ferroelectrics **104**, 147 (1990).

[2]J. Albers, A. Klöpperpieper, H. J. Rother, and K. Ehses, Phys. Status Solidi (a) **74**, 553 (1982).

[3]W. Schildkamp and J. Z. Spilker, Z. Kristallogr. **168**, 159 (1984).

[4]J. Albers, A. Klöpperpieper, H. J. Rother, and S. Haussühl, Ferroelectrics **81**, 27 (1988).

[5]M. L. Santos, J. C. Azevedo, A. Almeida, M. R. Chaves, A. R. Pires, H. E. Müser, and A. Klöpperpieper, Ferroelectrics **108**, 363 (1990).

[6]R. Böhmer, M. Maglione, P. Lunkenheimer, and A. Loidl, J. Appl. Phys. **65**, 901 (1989).

[7]U. T. Höchli, K. Knorr, and A. Loidl, Adv. Phys. **39**, 405 (1990).

[8]W. Känzig, H. R. Hart, Jr., and S. Roberts, Phys. Rev. Lett. **13**, 543 (1964).

[9]U. T. Höchli, Phys. Rev. Lett. **48**, 1494 (1982).

[10]E. Courtens, Phys. Rev. Lett. **52**, 69 (1984); Helv. Phys. Acta **56**, 705 (1983); Ferroelectrics **72**, 229 (1987); H. Terauchi, Phase Transitions **7**, 315 (1986); V. H. Schmidt, Ferroelectrics **72**, 157 (1987).

[11]K. Binder and A. P. Young, Rev. Mod. Phys. **58**, 801 (1986).

[12]J. Wong and C. A. Angell, in *Glass: Structure by Spectroscopy* (Marcel Dekker, New York, 1976).

[13]R. Kohlrausch, Ann. Phys. (Leipzig) **12**, 393 (1847); G. Williams and D. C. Watts, Trans. Faraday Soc. **66**, 80 (1970).

[14]I. Fehst, R. Böhmer, W. Ott, A. Loidl, C. Bostoen, and S. Haussühl, Phys. Rev. Lett. **64**, 3139 (1990).

[15]A. Loidl, K. Knorr, I. Fehst, R. Böhmer, J. Hessinger, and U. T. Höchli, J. Non-Cryst. Solids (to be published).

[16]C. A. Angell, J. Phys. Chem. Solids **49**, 863 (1988).

[17]M. Braune, Diplomarbeit, Universität Mainz, 1990 (unpublished); M. Braune, B. Mertz, and A. Loidl (to be published).

[18]K. L. Ngai, J. Non-Cryst. Solids **95&96**, 969 (1987).

[19]K. L. Ngai (private communication). In a recent paper on polymer blends it has been shown how site disorder must be appended to the coupling model: C. M. Roland and K. L. Ngai (to be published).

[20]K. Binder, Ferroelectrics **104**, 3 (1990); J. Non-Cryst. Solids (to be published), and references therein.

[21]G. Fischer, H. J. Brückner, A. Klöpperpieper, H.-G. Unruh, and A. Levstik, Z. Phys. B **79**, 301 (1990).

[22]S. R. Elliott, Adv. Phys. **36**, 135 (1987); A. R. Long, Adv. Phys. **31**, 553 (1982).

[23]M. Pollak and G. E. Pike, Phys. Rev. Lett. **28**, 1449 (1972).

[24]The CBH model was introduced by Pike to account for the dielectric loss in scandium oxide: G. E. Pike, Phys. Rev. B **6**, 1572 (1972).

[25]N. F. Mott, Rev. Mod. Phys. **80**, 203 (1978).